



D : 26

Work package No. :	05 (Carbon/Chlorophyll-a ratio)
Lead contractor:	HYD
Main objective:	Key processes Carbon-Chlorophyll-a ratio
Strategic leader:	Dr. Loga-Karpinska (WUT)
Responsible task leader:	Dr. Baumert (HYD)

Main contributors involved:	Organisation and E-Mail	
Dr. Baumert	HYD	baumert@hydromod.de
Dr. Levikov	HYD	levikov@hydromod.de
Dr. Frisk	PRC	tom.frisk@ymparisto.fi
Dr. Annu Peltonen	PRC	annu.peltonen@ymparisto.fi
Dr. Loga-Karpinska	WUT	malgorzata.loga@is.pw.edu.pl
Dr. Szeligiewicz	WUT	
Dr. Güde	ISF	hans.guede@ifula.lfu.bwl.de
Dr. Hollan	ISF	Eckard.Hollan@ifula.lfu.bwl.de
Dr. Wahl	ISF	isf.eurolakes@ifula.lfu.bwl.de

Dissemination level:

1 EXECUTIVE SUMMARY

This EUROLAKES Deliverable D26 summarizes studies and activities within EUROLAKES WorkPackage 05 on the role of the *Chlorophyll*-carbon ratio in large deep European lakes. To keep this document readable the partners involved in reporting concentrated their contributions on the very essence of the results and methods elaborated. Selected aspects are presented in ANNEX A to this deliverable on about 100 pages in sufficient detail.

The results achieved may be summarized as follows:

- The intracellular *Chlorophyll*-carbon ratio of phytoplankton plays an important role in the modelling of ecosystems of deep large lakes. It exhibits a high variability, mainly in time.
- The field observation of the *Chlorophyll*-carbon ratio in lakes is a highly sophisticated task. While Chlorophyll is easy to measure, the discrimination of carbon into phytoplankton and non-phytoplankton components is extremely difficult. Therefore explicit measurements for the lakes under study could not be found in the literature and could not be carried out within the framework of the EUROLAKES project. Instead we concentrated on the world-wide first comprehensive data set published just recently based on mesocosm experiments in North America, and on observations from Narragansett Bay, USA.
- The *Chlorophyll*-carbon ratio may be calculated by different means. A generic approach has been provided by HYDROMOD. Here the intracellular ratio is computed explicitly based on a mechanistic theory of cell division, photosynthetic Z-scheme and a carbon balance under the influence of light, temperature and the major nutrients **N**, **P** and **Si**. This theory-based approach gave excellent agreement with the mesocosm and Narragansett Bay data. The model has been successfully integrated into the complex Loch Lomond ecosystem model the results of which are reported in greater detail in the Final Report of EUROLAKES WorkPackage 22.
- Another approach to the intracellular *Chlorophyll*-carbon ratio was chosen by the partners WUT and PRC who computed that ratio implicitly using separate balance equations for the carbon compounds and the *Chlorophyll*. Their models capture basic features of phytoplankton growth in deep large lakes. They correctly simulate the appearance of spring phytoplankton blooms, subsequent clear water phases and the basic behaviour of light-limited growth in the mixed layer, as described in the literature for the lakes under study.
- Experience of WUT has shown that the most difficult problem is the correct determination of the mixing depth. The advantage of the arbitrary visual method proposed for the model consists in taking into account past mixing events retained in the temperature profiles in form of many sub-thermoclines. However such a procedure often does not lead to the unique solution, and is difficult and subjective, especially at the beginning of the stratification period.
- The results presented by WUT for 1996 show that a proper description of phosphorus and phytoplankton sedimentation is crucial for the modelling of lakes. A further challenge is the correct modelling of zooplankton and detritus which should be also simulated in greater detail.
- Despite of many simplifications the models presented seem to be a useful basis and a reference point for improvements and still more sophisticated constructions.

Table of Contents



	Eurolakes	1
1	Executive Summary	2
2	Introduction	5
3	Part I: Warsaw University of Technology	6
	Modelling the Lac du Bourget ecosystem	
3.1	GENERAL METHODOLOGICAL QUESTIONS	6
3.2	BRIEF GENERAL CHARACTERIZATION OF STUDY ECOSYSTEM.....	6
3.2.1	<i>Phytoplankton</i>	7
3.2.2	<i>Zooplankton</i>	8
3.2.3	<i>Phosphorus</i>	8
3.2.4	<i>Transparency</i>	9
3.3	PHYTOPLANKTON MODEL FOR LAKE BOURGET	9
3.3.1	<i>Description of the model</i>	9
3.3.2	<i>Input data</i>	11
3.3.3	<i>Model results</i>	11
3.4	SUMMARY AND CONCLUSION	17
3.5	APPENDIX 1	18
3.6	APPENDIX 2	18
3.7	APPENDIX 3	19
3.8	LIST OF SYMBOLS USED IN CHAPTER 3	20
4	Part II: HYDROMOD Scientific Consulting	21
	Theory of the Chlorophyll-carbon ratio and integrated water-column modelling	
4.1	INTRODUCTION	21
4.2	OVERVIEW	21
4.2.1	<i>Coupling of plankton and turbulence</i>	21
4.2.2	<i>Integrated biological-physical modelling</i>	22
4.3	SELECTED RESULTS	22
4.3.1	<i>Coupling of plankton and turbulence</i>	22
4.3.2	<i>The physiological submodel: constant temperature</i>	23
4.3.3	<i>The physiological submodel: variable temperature</i>	24
4.3.4	<i>The hydrophysical submodel</i>	26
4.4	INTEGRATED BIOLOGICAL-PHYSICAL MODELLING	27
5	Part III: Pirkanmaa Regional Environment Centre	
	Calculation of nutrients, phytoplankton biomass and chlorophyll-a	
5.1	INTRODUCTORY NOTE	29
5.2	PHOSPHORUS	29
5.3	NITROGEN.....	30
5.4	CHLOROPHYLL	31
5.5	CARBON-BASED BIOMASS	32
5.6	BIOLOGICAL AVAILABILITY OF NUTRIENTS.....	33

5.7	LIGHT LIMITATION AND LAKE OPTICS	34
5.8	TEMPERATURE AND MATTER CONVERSION RATES.....	35
5.9	ZOOPLANKTON	36
5.10	SUPPLEMENTING STATISTICAL MODELS	38
6	list of references	38

2 INTRODUCTION

In the following the contributions of three partners of EUROLAKES WorkPackage 05 are summarized. These are WUT, HYDROMOD and PRC. The further partner ISF involved also in this WorkPackage supported our work mainly in form of comments, criticism and advice *sensu an advocatus diaboli*. Although not explicitly visible, this important ISF contribution shall here be highly acknowledged. We particularly thank Hans Güde, Eckhard Hollan and Bernd Wahl for interesting discussions and their indispensable advice.

3 PART I: WARSZAW UNIVERSITY OF TECHNOLOGY

Modelling the Lac du Bourget ecosystem¹

3.1 GENERAL METHODOLOGICAL QUESTIONS

Studying phenomena in very deep and large lakes as the EUROLAKES are, there is a need to analyse all relevant processes i.e. processes of physical, chemical and biological character in proper time scale, spatial scale and proper dimension perspective.

Knowing that lac du Bourget similarly to lake Constance, lake Geneva do not mix every year but, taking statistically every second year lac du Bourget become a real challenge for scientist hydrologist and limnologist to understand and simulate the behaviour of its ecosystem.

Having much experience with using TELEMAC system for modelling shallow Zegrzyński reservoir in central Poland where TELEMAC 2D was used for simulating hydrodynamic and SUBIEF 2D for simulating the ecosystem of the reservoir, in particular eutrophication of this reservoir the TELEMAC system has been chosen as a tool for studying dynamics of the lake Bourget. Unfortunately during the span of the EUROLAKES project three dimensional version of this software was available only for hydrodynamic modelling. So instead of envisaged 3D modelling of the lake Bourget ecosystem only much simpler simulations could have been performed. It has been decided to concentrate on processes of algae dynamics with interrelation of vertical mixing, water temperature profile, light climate (attenuation profile), grazing force of zooplankton.

3.2 BRIEF GENERAL CHARACTERIZATION OF STUDY ECOSYSTEM

Lake Bourget is located in the French Alps in Savoie and is a biggest natural lake situated on the French territory. Bourget lake is situated in the vicinity of two important cities: Chambéry and Aix les Bains (400 000 inhabitants – equivalents).

Table 3.1: Bathymetric and hydrologic characteristic of lake Bourget

Bathymetric and hydrologic characteristic of lake Bourget	Value /units
Length of the lake	18 km
Maximum width	3,2 km
Water surface area	44.6 km ²
Mean depth	81 m
Maximum depth	145 m
Volume	3,6 x10 ⁹ m ³
Shoreline length	43,3 km
Theoretical retention time	7 years

¹ Authors of PART I:

Dr *Wojciech Szeligiewicz* from Polish Academy of Sciences

Dr *Małgorzata Loga-Karpińska* from WUT

Western part of the lake catchment is very steep and consist of bed rock. Eastern shore is much more flat and transformed by people living in small villages and towns. Lake Bourget serves as drinking water reservoir for Aix –les-Bains.

Catchment of lake Bourget consists of six sub-catchments. Five of these sub-catchments are catchments of main inflows to the lake i.e. Leysse, Belle Eau, Sirroz, Tillet and Chautagne rivers. The last sub-catchment does not have main inflow.

In the upper part of Leysse catchment rural areas with cattle farming are dominating together with forests. While the lower part of the catchment is much more heavily populated, urbanized and industrialised.

Since the beginning of 60'ties lake has been suffering from eutrophication.

Recently two year survey (1995-96) had been carried out in the lake. The diversion of the main waste water discharge since the beginning of the 80'ties has caused reduction of phosphorus and nitrogen loading by 50% and 70 % respectively. As a consequence, the concentration of phosphate in winter decreases by 70% and nitrogen by 25%. An observed decrease of the nutrients concentration in the water column is most likely not simply a result of reduction of external loading but also is caused by an increase of sedimentation of phosphorus associated with organic detritus.

Values of some water quality elements measured during above mentioned survey show improvement of lake water quality in comparison to the previous survey performed in 1988-89. However water quality elements like chlorophyll-a concentration, algae species composition and abundance still indicate eutrophication.

Since 90' orthophosphate and nitrogen concentrations in the water column reveal some stabilization. It is probably caused by internal nutrient loading from the lake sediments occurring under anoxic conditions at the lake bottom.

There are some symptoms of improvement of water quality observed as "clear water phase" and increase of dissolved oxygen concentration at the thermocline.

Two physical characteristics are of special importance. The first is the maximum depth of the lake which does not allow a yearly complete overturn. Therefore, Lake Bourget is a meromictic one. The second physical characteristic is the mean residence time, which allows only for small year to year changes in the ecosystem characteristics, apart of the effect of meteorological forcing.

3.2.1 Phytoplankton

When comparing the phytoplankton data collected in 1988-89 and 1995-96 it can be observed that despite the total amount of blue-greens decrease the concentration of dominant blue-green species is still high as characteristic for eutrophic waters. There were 162 species of algae identified in Bourget lake in 1995/96.

Blue-greens were present through all the year 1995 and 1996 with a maximum in August. The most abundant among all of them were *Oscillatoria limnetica*, *Aphanizomenon flos aquae* and *Oscillatoria rubescens*.

All nannoplankton and microplankton species present in the lake during these two years develop simultaneously in contrary to other subalpine lakes where nannoplankton species develop in spring and other species during the rest of the year.

Mean chlorophyll a concentration for the 10 m surface layer is 8.6 µg/l in 1995 and 6.7 µg/l in 1996. Seasonal variation of chlorophyll-a follows the dynamics of diatoms and greens with maximum in April/May and second maximum in August (Fig.3.1)

3.2.2 Zooplankton

Data concerning biomass of zooplankton (rotifers and crustaceans) for 1995 and 1996 are shown in Fig. Crustacean zooplankton in this lake is represented mainly by herbivore organisms. However, in case of lake Bourget, they feed rather on decomposers (bacteria) as well as on unicellular detritivores or organic matter resulted from degraded phytoplankton and zooplankton.

3.2.3 Phosphorus

The dynamics of the ratio phosphorus/nitrogen in water (from 6.67 in 1981 to 17.6 in 1996) show that phosphorus is a limiting factor for primary production in the lake. The high trophic status is caused by excessive phosphorus concentration in the water (0.034mg/l of phosphate phosphorus).

Sudden variations of orthophosphate phosphorus in the water column within the time scale of months are frequently observed. These events, cannot be explained solely by primary production or mineralisation. They are probably related to the flood events in the inflowing rivers.

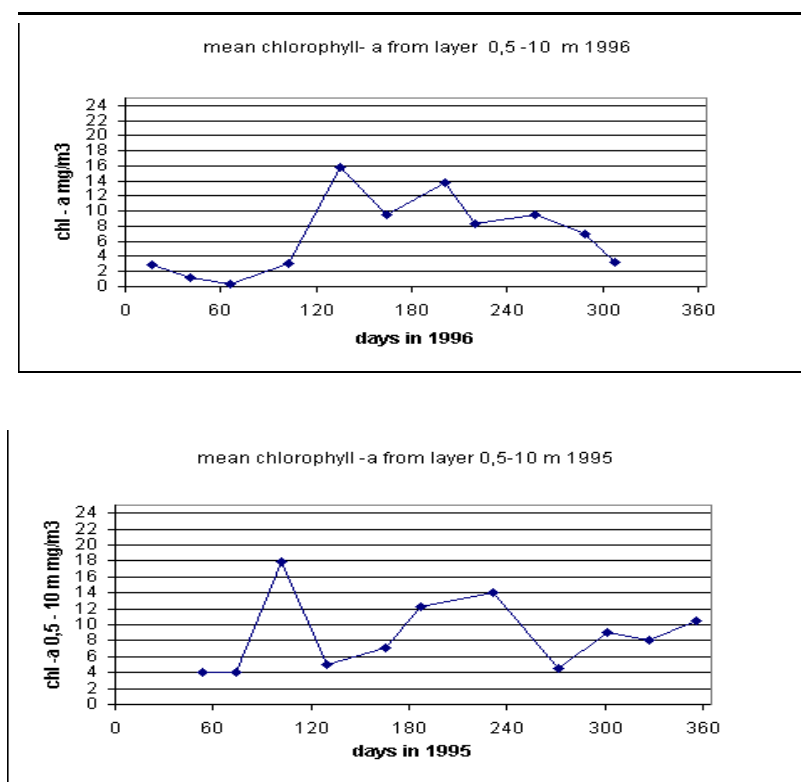


Figure 3-1

Variation of chlorophyll-a concentration in 1995 and 1996 mean values for the 0,5-10m layer

3.2.4 Transparency

Mean water transparency value for the period April- September is 3,5 to 4,5 m. Biggest transparency has been observed in May 1995 on 25 during the "clear water phase" Maximum measured transparency in winter is about 15m. The transparency decreases in result of phytoplankton spring bloom. It increases again in Mai-June as a response to zooplankton grazing when zooplankton reduces phytoplankton concentrations and clear water phase begins. Minimal values are reached during the summer production - 1.8 m in June/July.

3.3 PHYTOPLANKTON MODEL FOR LAKE BOURGET

The aim of the model is to contribute to the understanding of phytoplankton dynamics in this lake and to prepare a starting point to the further, more sophisticated, 3D modelling of the ecosystem.

The model is based on one-dimensional approach: it is assumed that only vertical mixing is responsible for transport of dissolved and particular matter. This approach is justified only when the typical time scales for transformation and for vertical mixing processes are much larger than the time needed for horizontal mixing.

In addition, well mixing condition was assumed for the upper most water layer of the lake. It means that all particles and dissolved substances are uniformly distributed throughout this layer. This kind of approach enables to simplify the examination of the influence of vertical mixing on the functioning of the ecosystem. The latter approach appeared to be very fruitful in theoretical as well as practical implementations of models concerning phytoplankton biomass under well-mixed conditions (e.g. Huisman and Weissing, 1994, Szeligiewicz 1998, Sverdrup 1953) and may be used as a first approximation at least to the stratified water bodies.

The model is designed to fulfil the following requirements:

- It should be kept as simple as possible in order to facilitate the development of 3D version.
- It should represent the integrated algal biomass.
- The model should take into account all key factors influencing phytoplankton biomass growth in the lake
- The model should reproduce and the principal features of the dynamics of phytoplankton biomass (time and intensity of phytoplankton blooms) or at least it should assist further development.

3.3.1 Description of the model

The model describes phytoplankton biomass dynamics of the surface layer of the 50 m depth. The depth of this layer is adopted arbitrarily to include seasonal vertical water stratification and principal mixing events at the water surface, and to catch main vertical changes in the most limiting factors of primary production (see Fig.3.0 for examples of temperature profiles). The layer is divided into 50 sub-layers of 1m depth and local growth conditions within the sub-layers are assumed. The most upper part of this layer is assumed to be well-mixed.

Eurolakes Deliverable:	D26
From Workpackage:	WP 05
FP5_Contract No.:	EVK1-CT1999-00004
Version:	
Date:	20.10.03

Phytoplankton growth in the model is phosphorus-limited according to the report on field measurements and furnished with data. The growth depends also on light, temperature and zooplankton grazing (see APPENDIX 2).

All phytoplankton species presented in the lake are aggregated into one group of photosynthesising organisms described by a single set of parameters for a given year. Temporal changes in the values of these parameters resulted e.g. from seasonal phytoplankton succession are not considered.

Phytoplankton biomass for a given day is calculated from a biomass balance for each of the sub-layers for that day. Then, biomass distributed in upper part of the layer is averaged at the end of the day depending on the depth of well-mixed layer. The depth is assessed from temperature profiles or calculated from mechanic energy balance (optionally) according to the admitted mixing conditions (APPENDIX 3). If the depth of the well-mixed layer increases then the biomass from the lower sub-layers involved into the actual full mixing processes is entrained into the well-mixed layer.

Water currents due to rivers inflow are neglected. Lake bathymetry is not considered. Phosphorus and zooplankton concentrations are forcing variables. Water transparency is not a forcing variable in this model. Inversely, the transparency is calculated as a function of chlorophyll content in the water. In such way self-shading becomes the only mechanism of self-regulating mechanism of phytoplankton growth and phytoplankton biomass in the model.

Model calculations have been performed for two consecutive years: 1995 and 1996 for which field measurements were available.

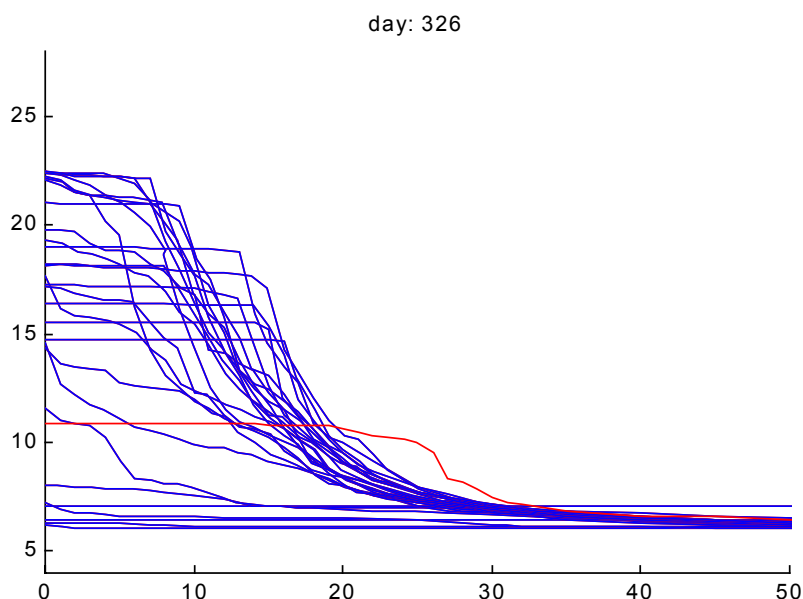


Figure 3-2.
Temperature profiles measured in the lake Bourget in 1996.
Red line corresponds to the profile on 326 day of the year. Vertical axe
refers to temperature and horizontal axe to depth below water surface.

3.3.2 Input data

The model requires data on water temperature profiles, phosphorus profiles, zooplankton and meteorological data: solar radiation and wind speed. Biological and physical parameters were taken from literature as the starting values for model calibration. The measurements on phytoplankton biomass were also necessary in order to verify and calibrate the model. The data used for this study are from the two year survey 1995/1996. Water temperature measurements are shown in Fig.3.0 (T profiles). The schematic diagram of the model has been shown in Fig.3.1. The data on phosphorus and zooplankton measurements as well as on surface temperatures and calculated mixing depths are depicted along with the model results in order to facilitate the analysing the calculated results of simulations. It was necessary to calculate the solar radiation as a function of day of the year and insolation (APPENDIX 1) in Fig.3.2.

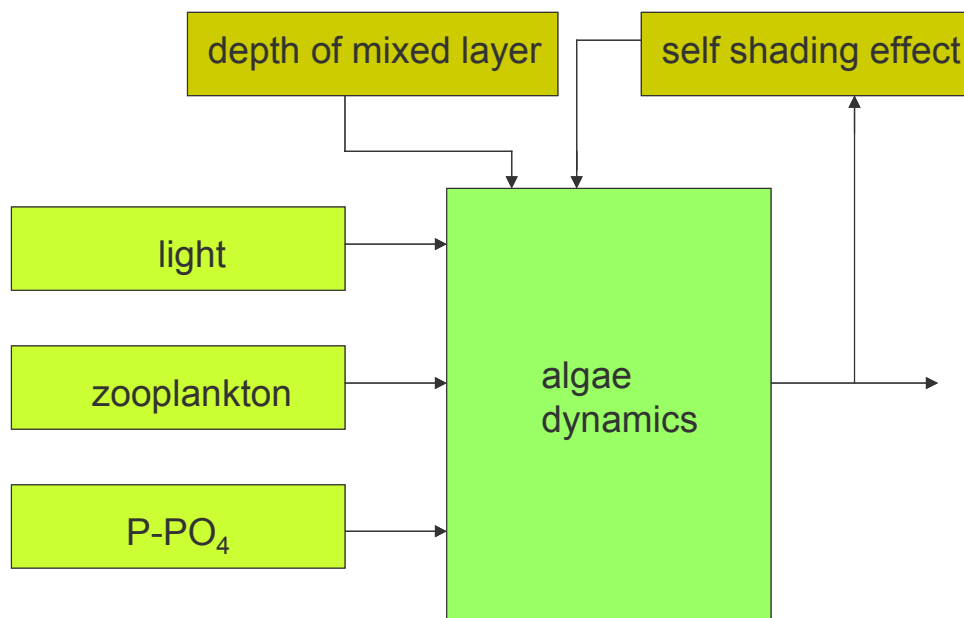


Figure 3-3
Fig.3.1. Block diagram of phytoplankton model

3.3.3 Model results

Simulations have been performed for two periods of 250 days of 1995 and 1996. This period has been chosen for simulation due to pronounced stratification of the 50m depth's surface layer. Phytoplankton biomass calculated is expressed the model by chlorophyll-a concentration. Results for 1995 are shown in Fig.3.3.a together with measured vales of chlorophyll-a concentration. The references of the result to input data dynamics (Fig.3.3.b, 3.3.c, 3.3.d, 3.3.e and Fig.3.2.a) suggest that the spring bloom observed in the lake in 1995 probably is an integrated result of high phosphorus concentration in the water, sudden increase of water temperature and better light conditions. Clear water phase following the bloom is a consequence of zooplankton

grazing and phosphorus depletion, deterioration of weather conditions (lower radiation, higher wind speed) resulted in increasing of mixing depth and decreasing of water temperature. Interestingly, there are other, summer blooms calculated which were not detected by the field measurements. Finally, calculated as well as observed phytoplankton concentrations decrease at the beginning of the autumnal overturn.

The simulations performed for 1995 show sudden decrease of the chlorophyll concentration after the spring bloom, not supported by the field data (Fig.3.4.a). It is due to the total exhaustion of phosphate phosphorus in the uppermost layers as observed in field measurements (Fig.3.4.b) and from zooplankton grazing (Fig.3.4.c). Note, that zooplankton grazing is already about four time smaller for this calculations than for the Fig.3.3 (see list of

symbols). Assuming the minimum phosphate phosphorus concentration not smaller than 1 mg/m³, in the uppermost layers, the same calculation leads to the result shown in Fig. 3.5, more consistent with field measurements. The latter assumption may reflect a supposition that below certain threshold value of phosphorus concentration cannot decrease. Models may easily facilitate this assumption. Another possibility is to assume that phytoplankton may grow in these conditions due to internal nutrients storage. This approach has been not included the model.

Fig.3.6 shows the model results in case of mixing depth calculated from criteria based on mechanical energy balance (see APPENDIX 3).

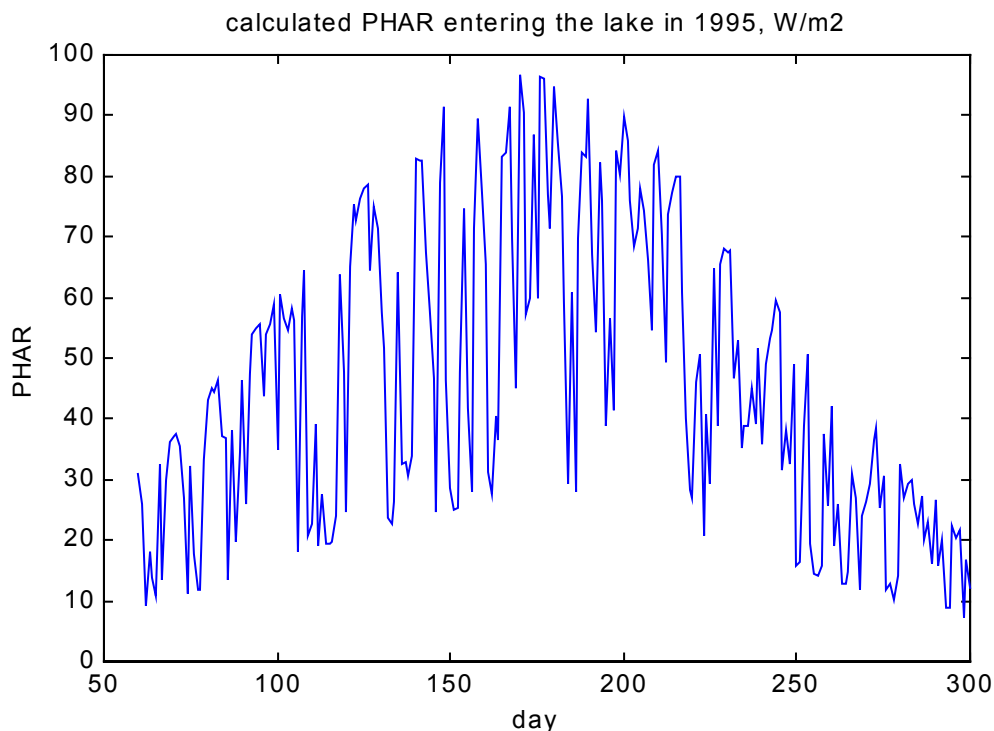


Figure 3-4a
Photosynthetically available radiation calculated for 1995 for lake Bourget

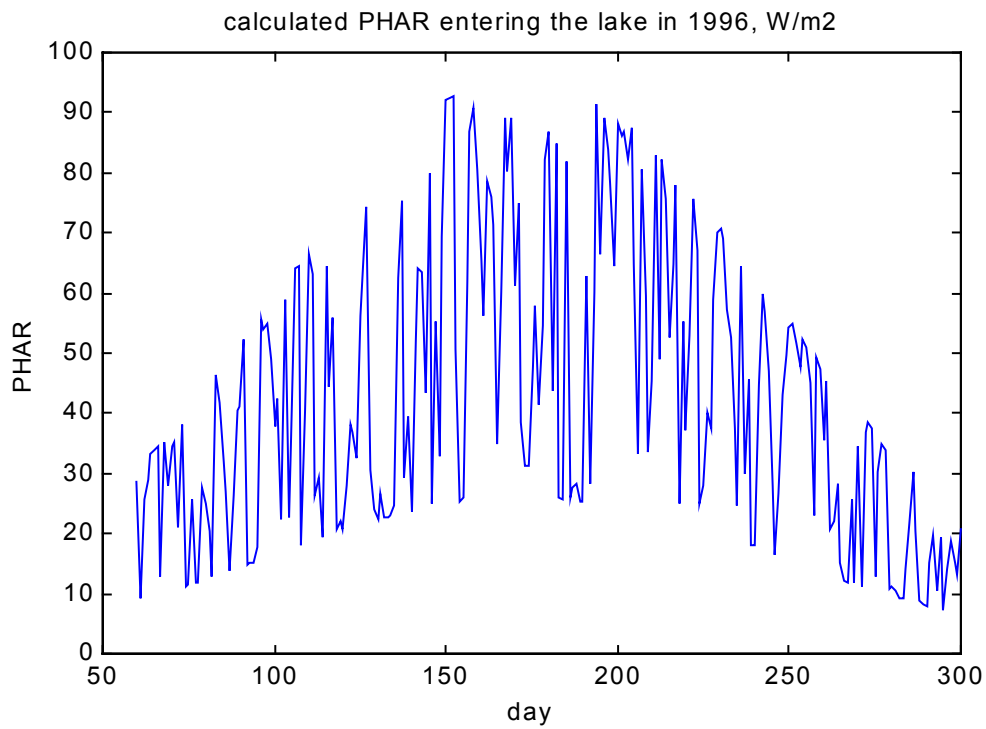


Figure 3-4b
Photosynthetically available radiation calculated for 1996 for lake Bourget

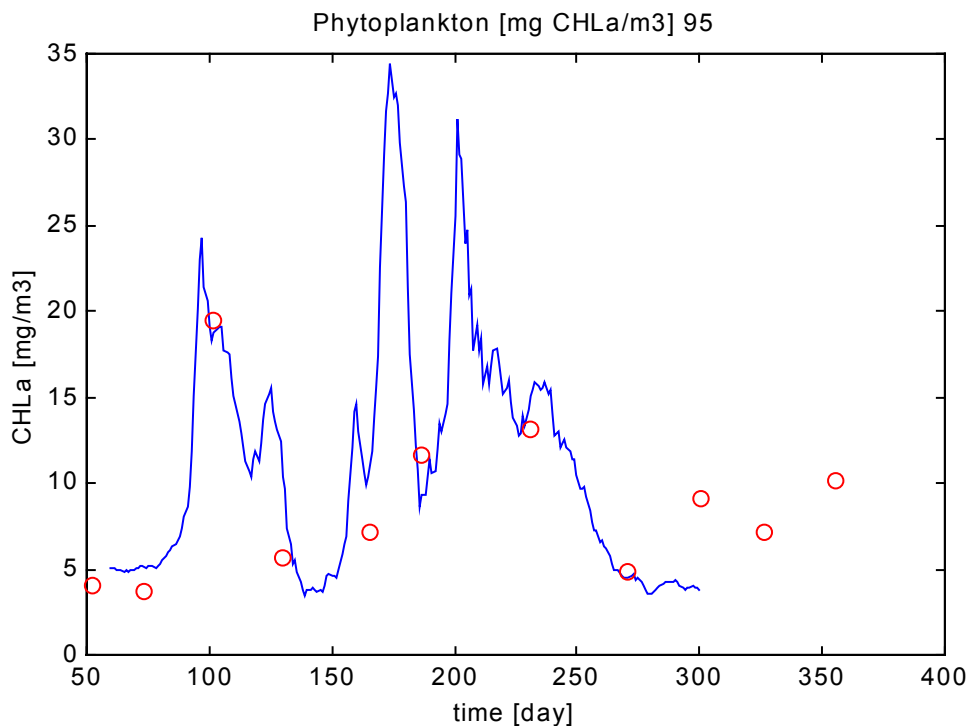


Figure 3-5a. Calculated chlorophyll a concentration in the mixed layer in 1995 for lake Bourget. Red circles denote measurements.

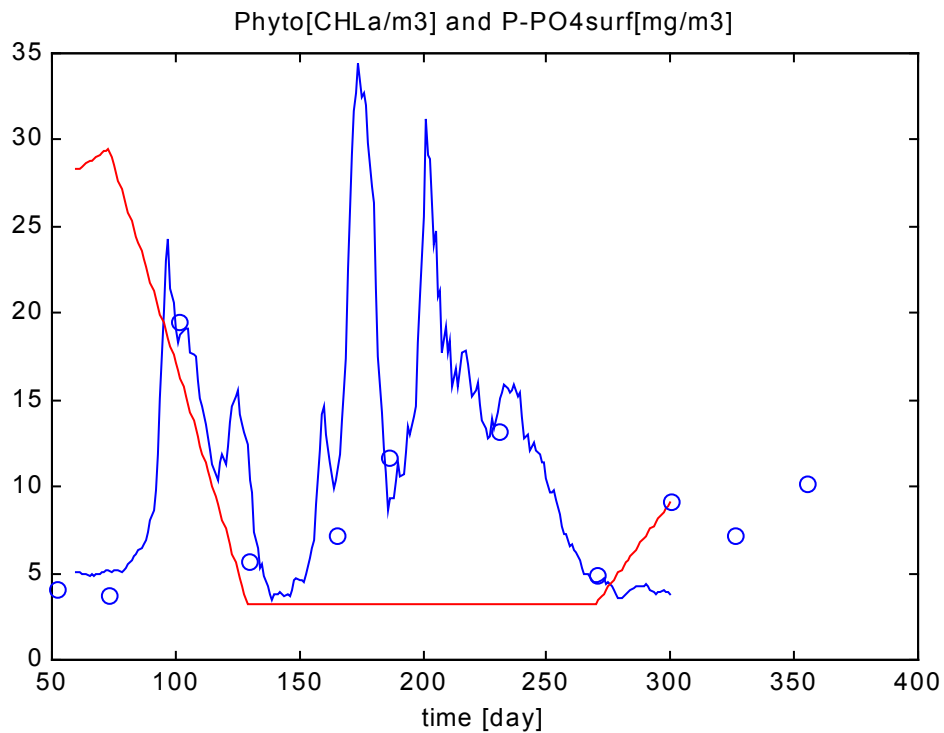


Figure 3-5b. Calculated chlorophyll a concentrations (blue line) and measured phosphate-phosphous concentrations (red line). Blue circles denote chlorophyll a measurements

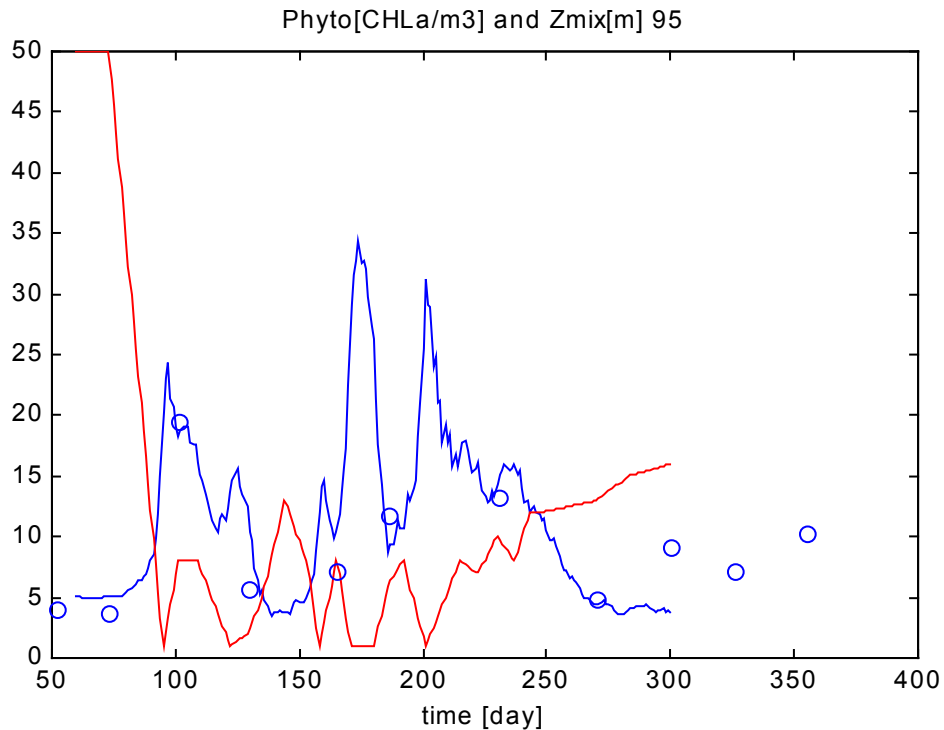


Figure 3-5c. Calculated chlorophyll a concentrations (blue line) and mixing depths (red line). Blue circles denote chlorophyll a measurements.

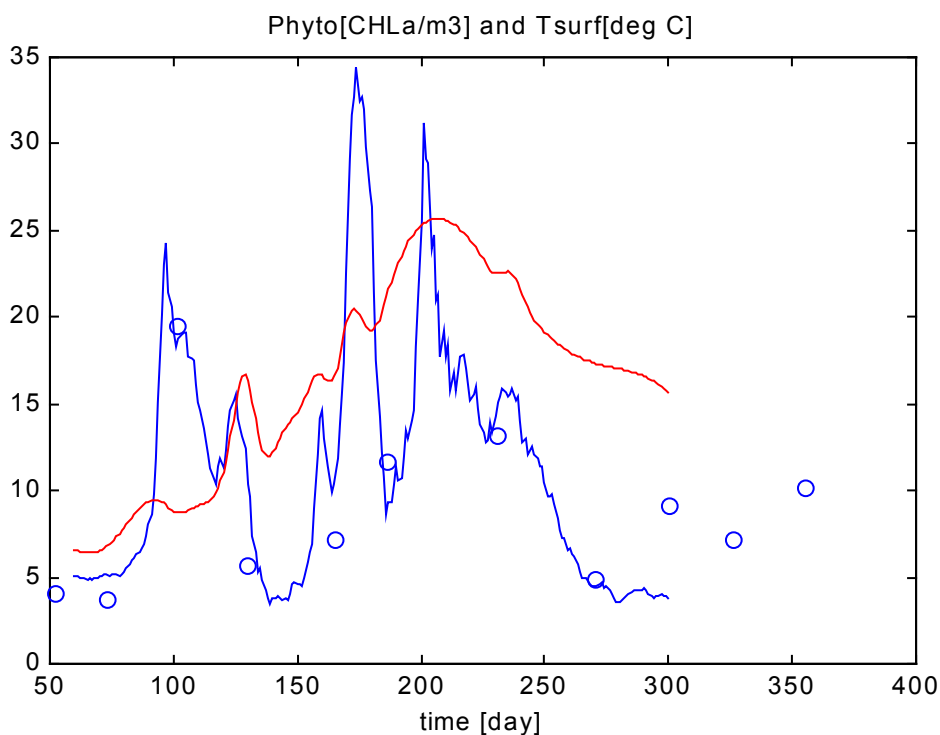


Figure 3-5d. Calculated chlorophyll a concentrations (blue line) and measured surface temperatures in 1995 (red line). Blue circles denote chlorophyll a measurements.

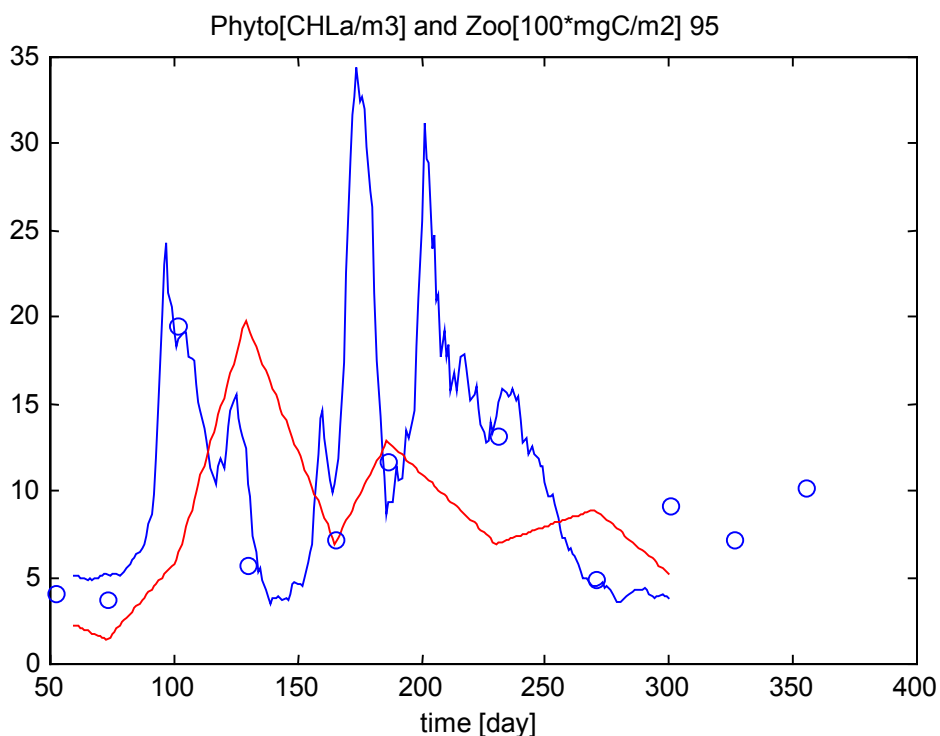


Figure 3-5e. Calculated chlorophyll a concentrations (blue line) and measured zooplankton concentrations (red line). Blue circles denote chlorophyll a measurements.

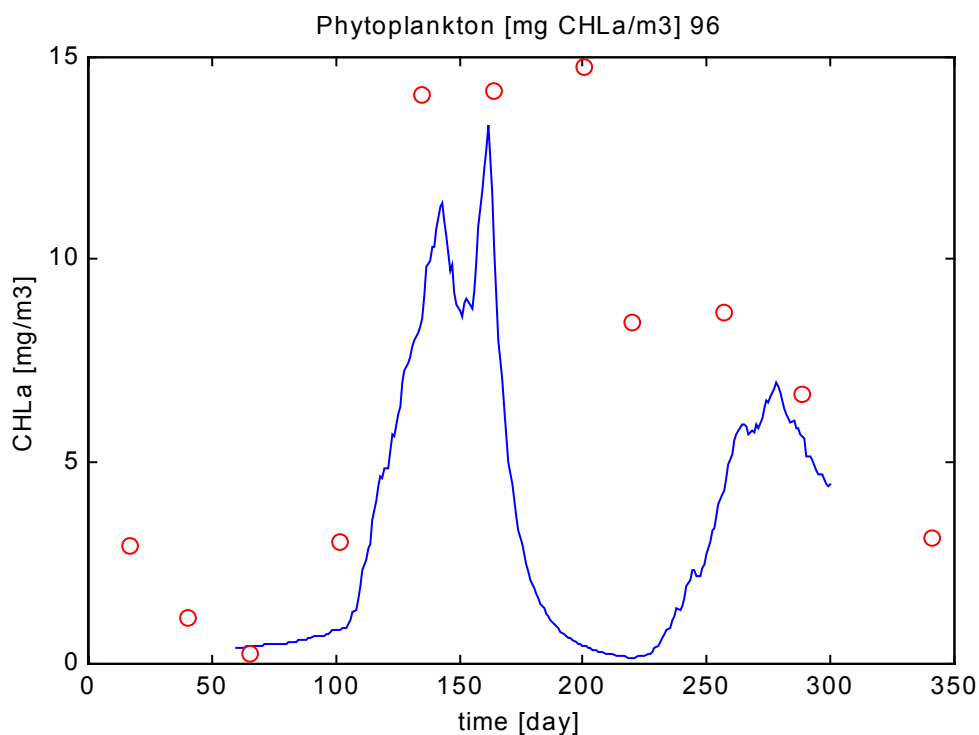


Figure 3-6a. Calculated (blue line) and measured (red circles) chlorophyll a concentrations in 1996.

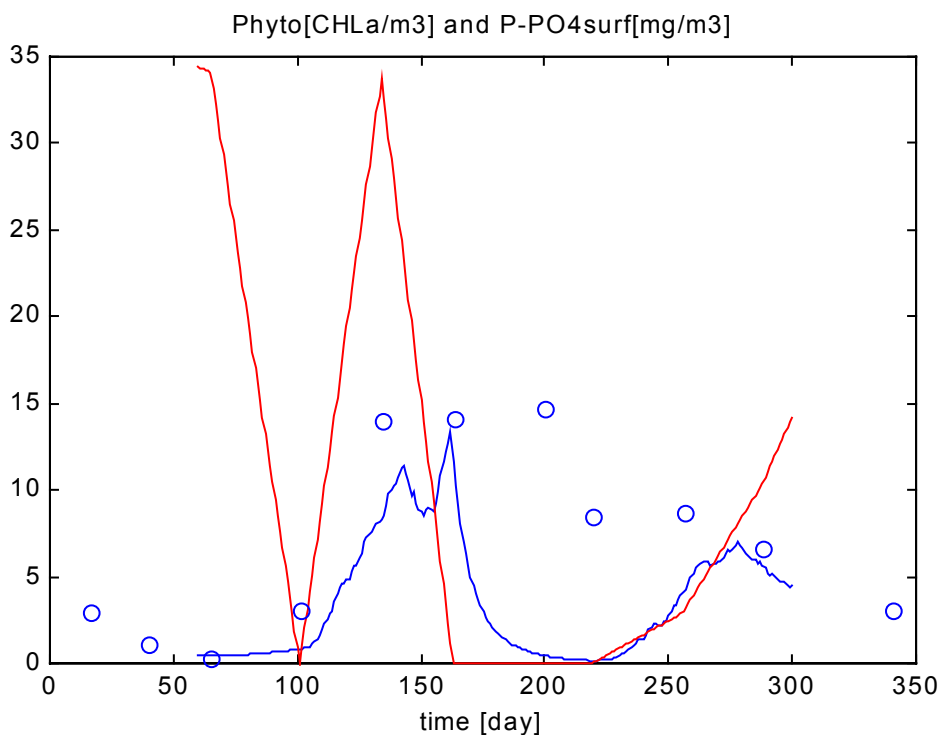


Figure 3-6b. Calculated chlorophyll a concentrations (blue line) and measured phosphate phosphorus concentrations (red line) in 1996. Blue circles denote chlorophyll a measurements.

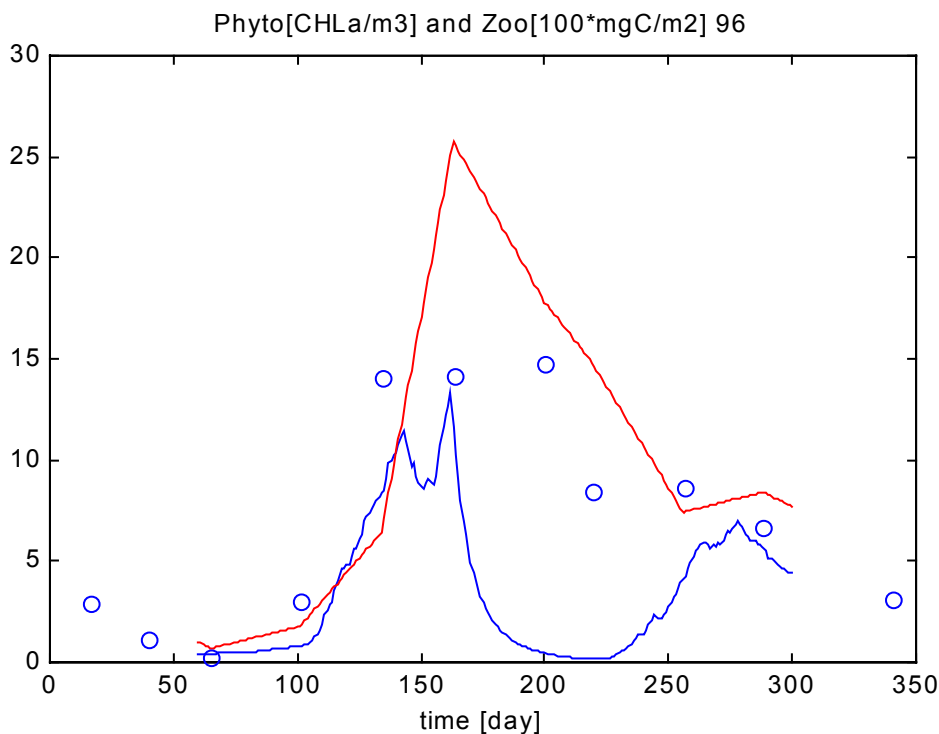


Figure 3-5c. Calculated chlorophyll a concentrations (blue line) and measured zooplankton concentrations (red line) in 1996. Blue circles denote chlorophyll a measurements

3.4 SUMMARY AND CONCLUSION.

The model presented in this report captures basic features of phytoplankton growth in the lake Bourget. It correctly qualitatively simulates the appearance of spring phytoplankton bloom and subsequent clear water phase. In addition, it retains basic behaviour of light-limited growth in the mixed layer, described qualitatively by Huisman and Weissing (1994), Weissing and Huisman (1994) and Szeligiewicz (1998).

The most difficult problem in the model concerns determination of mixing depth. The advantage of the arbitral visual method proposed in the model consists in taking into account past mixing events retained in the temperature profiles in form of many sub-thermoclines. However such a procedure often does not lead to the unique solution, and is difficult and subjective, especially at the beginning of stratification period. While calculations of the mixing depth based on energy balance concern only the day for which temperature profile is measured. The best situation would be if temperature profiles were available for each day of simulations. The more adequate method is to apply a hydrodynamic model simulating vertical mixing and couple it with biological sub-model. However, it would be the lost of the model simplicity.

The results presented above, especially for 1996, show that phosphorus should be also modelled. A proper description of phosphorus and phytoplankton sedimentation may appear a crucial problem in the modelling of the lake. Moreover, the phosphorus stored inside phytoplankton

cells should be included in order to simulate phytoplankton growth in periods of lacking this element in the surrounding water. Different phytoplankton classes that could be considered in the model may further improve the results. Finally, zooplankton and detritus should be also simulated.

Despite of many simplifications the model seems to be a useful tool as a reference point for more sophisticated construction.

3.5 APPENDIX 1

Solar radiation is calculated according to standard equations published in literature (e.g. Gaillard 1981, Henderson-Sellers 1987, Kirk 1983, Lafforgue 1990, Tassin 1986).

3.6 APPENDIX 2

Phytoplankton growth is calculated from a balance between primary production and phytoplankton losses:

$$\frac{dF}{dt} = (p - l)F \quad (3.1)$$

where F represents phytoplankton biomass concentration, p is the specific (per unit phytoplankton biomass) primary production and l is the specific biomass losses.

Specific primary production (p) is expressed by a Monod function of light intensity (I):

$$p = p_{\max} \frac{I}{I + L} \quad (3.2)$$

where L is the half saturation constant for light-limited production, and p_{\max} is the maximum specific production rate. Light intensity (I) at the depth (z) in the water depends on the light supply to the water (I_0) and is described according to Lambert_Beer's law:

$$I(z) = I_0 e^{-\varepsilon z} \quad (3.3)$$

where ε is the light extinction coefficient of water, and depends on the phytoplankton concentration:

$$\varepsilon = kF + K_{bg} \quad (3.4)$$

where K_{bg} is the background attenuation coefficient.

Primary production expressed by eq.2 increases asymptotically to the value p_{\max} as I increases. This equation does not include photoinhibition effect. Primary production is subsequently diminished multiplying right hand side of eq.2 by a Monod function of local nutrient concentration. Since primary production is limited by phosphorus in this lake in 1995 and 1996 according to the report on field measurements furnished to this study, the algal production is:

$$p = p_{\max} \frac{I}{I + L} \frac{DP}{DP + K_{DP}} \quad (3.5)$$

Here, DP is the phosphate phosphorus concentration, and $K_{P_{O_4}}$ is the half saturation constant describing phosphorus-limited primary production. Assuming well-mixed condition for each of the sub-layers and integrating eq.3 over depth of the sub-layer, total primary production inside a sub-layer is:

$$p = \frac{p_{\max}}{\varepsilon} \frac{DP}{DP + K_{DP}} \frac{\ln I_1 + L}{\ln I_2 + L} \quad (3.6)$$

Here, I_1 and I_2 refer to the light at the upper and lower limit of the sub-layer.

Temperature dependence of the maximum specific production rate is expressed by:

$$p_{\max} = p_{\max 20} \exp(k_T(20 - T)) \quad (3.7)$$

where T is the temperature of water.

Specific phytoplankton losses (3.1) are described by

$$l = l_{bg} + gr \quad (3.8)$$

Here l_{bg} are the background specific phytoplankton losses, and gr are the specific losses due to zooplankton grazing, where

$$l_{bg} = l_{bg 20} \exp(k_T(20 - T)) \quad (3.9)$$

Zooplankton grazing in a sub-layer, i , is proportional to the zooplankton concentration in this sub-layer, $Z(i)$, and to a proportional coefficient, GR .

Vertical zooplankton distribution conforms to the vertical phytoplankton distribution in the following way:

$$Z(i) = BZ * F(i)/BF \quad (3.10)$$

where BZ is the zooplankton biomass in the water column, BF is the phytoplankton biomass in this column and $F(i)$ is the phytoplankton concentration in the sub-layer (i). Finally:

$$gr = GR * BZ * F(i)/BF \quad (3.11)$$

3.7 APPENDIX 3

The procedure of wind induced mixing is based on *Stefan and Ford (1975)* algorithm. According to this procedure, the wind-induced water currents lead to fully mixed surface layer

approximating to the epilimnion. The wind mixing algorithm refers to the balance of energy from the currents and energy necessary for mixing some upper layers. The latter energy depends on the mass differences and the distance between these layers. The layers can be mixed if the wind energy is high enough.

Apart from the full mixing of the most upper layers there is a possibility (optionally) of a "background" vertical turbulence diffusion of simulated matter .

3.8 LIST OF SYMBOLS USED IN CHAPTER 3

Symbol	Units	Definition	Values for Fig.3	Values for Fig.4	Values for Fig.5
p_{max20}	mg Chla /m ³ /d	Maximum specific production rate of biomass at 20°C	1	0.8	0.6
L	W/m ²	Half saturation constant for light-limited production	24	24	24
GR	mg Chl a /mg C/m/d	Grazing rate	0.002	0.0005	0.0005
K_{DP}	mg P-PO ₄ /m ³	Half saturation constant for phosphorus-limited production	0.5	0.5	0.5
l_{bg20}	d ⁻¹	Background loss rate of biomass at 20°C	0.03	0.03	0.03
k	m ² /mg Chl a	Specific light attenuation coefficient of biomass	0.03	0.03	0.03
K_{bg}	m ⁻¹	Background light attenuation coefficient	0.15	0.15	0.15
k_T	(°C) ⁻¹	Temperature dependence coefficient	0.046	0.46	0.46
I	W/m ²	Light intensity			
F	mg Chl /m ³	Phytoplankton concentration			
DP	mg P-PO ₄ /m ³	Phosphate-phosphorus concentration			
Z	mg C/m ²	Zooplankton concentration			

4 PART II: HYDROMOD SCIENTIFIC CONSULTING

Theory of the Chlorophyll-carbon ratio and integrated water-column modelling²

4.1 INTRODUCTION

The research project EUROLAKES is funded by the EC within the Fifth Framework Programme. It is an interdisciplinary study of lakes and their catchments, including the study of key processes like the role of the *Chlorophyll*-carbon ratio using recent advances in biophysical theory and numerical modelling.

Below we report selected advances made by HYDROMOD on this topic, including selected results of a new theory and numerical modelling approach for the coupling between phytoplankton and hydrophysics in lakes (EUROLAKES WorkPackage 05), and contributions to an improved integrated biological-physical modelling of the water column.

In the present document only an overview can be given. Technical details and the full range of theoretical derivations, mathematical tools and achieved results are documented in Annex A to this EUROLAKES Deliverable D26 which is available from HYDROMOD for the interested reader on request.

4.2 OVERVIEW

4.2.1 Coupling of plankton and turbulence

Within the circle of scientific problems around the coupling of plankton and turbulence the problem of light-dark adaptation of phytoplankton cells and their intracellular Chlorophyll-carbon ratio is a long-standing challenge to the biophysical sciences as those cells move along stochastic (turbulent) trajectories within an inhomogeneous underwater light field. This problem could be solved using a fundamentally new method for treating mathematically the coupling of slow physiological, intracellular plankton variables (with characteristic times of a couple of hours) with the ambient stochastic physics. We namely treated the cell trajectories as *Langevin equations* where the statistical properties of the noise are computed from a turbulence model like the one described above. The Langevin equations are then transformed into *Fokker-Planck equations* describing the evolution of the statistical properties of the solutions of the Langevin equa-

² Author of PART II:
Dr. *Helmut Baumert*

tions. Finally the Fokker-Planck equations are integrated over selected axes of the state space and for the remaining integrated equations a numerical solution algorithm has been elaborated and tested.

This is a *qualitatively new approach* in computational limnology.

We mention that smaller parts of the advances made here in relation to the coupling problem could be elaborated within the EC project PROVESS where this problem also played a key role.

4.2.2 Integrated biological–physical modelling

The work on the improvement and stepwise completion of an existing “mechanistic” model for phytoplankton photosynthesis published some years ago and based on a broad data set from four different phytoplankton species has been continued. Below we present selected results which show the model performance in relation to changes in the ambient temperature and their effect on the photosynthesis-light relation. This part of our work supplements and completes the approach described under "Coupling of plankton and turbulence" in so far as now also the temperature dependence of the cell's enzymatic chemistry is taken into account by the final model.

4.3 SELECTED RESULTS

4.3.1 Coupling of plankton and turbulence

In the pelagial of natural water bodies hydrophysical and hydrobiological processes are often closely coupled. Prominent examples are:

- Phytoplankton cells with inert internal variables like the *Chlorophyll*-carbon ratio, γ ; it is controlled both by the slow photoadaptation of the cell (integrating the experienced light over a longer time) and by irregular vertical movements in the underwater light field due to turbulence.
- SPM flocs (marine or lake snow) which represent relatively autonomous micro-ecosystems; the stickiness of their constituents is mainly governed by biology whereas their formation and breakup are controlled by the hydrophysical microstructure of the ambient water body.

Further examples are multiple-layer formation and convection due to light absorption by phytoplankton in deep levels, modulation of encounter and performance probabilities for zoo- and phytoplankton by turbulence and the formation of lutoclines or fluff layers near the bottom.

In numerical models the above aspects are often strongly simplified: If phytoplankton photoadaptation is discussed at all, it is done in a heuristic, semi-empirical way. If flocs are considered at all, they are mostly treated as static entities.

Based on the stochastic calculus of Langevin and Fokker-Planck equations a new solution for the Chlorophyll-carbon rate adaptation is presented which is important also for the treatment of flocculation problems which will not be discussed here in detail.

As to the dynamic effects of changing light intensity for phytoplankton cells, there are two main processes to be distinguished: (i) A short-term internal energy storage in the primary photosynthetic pathway; it has a time scale of (maximum) 100 seconds. (ii) The slow photoadaptation process with a time scale of at least 4 hours.

The role of the two effects in the upper mixed layer (UML) in the ocean with UML depth H [m] and vertical turbulent diffusivity D [$\text{m}^2 \text{s}^{-1}$] can easily be evaluated by the following similarity number, $p = \sqrt{\tau \cdot D} / H$, where τ [s] is the time scale of the biological process considered.

With $H = 25$ m, $D = 10^{-4} \text{m}^2 \text{s}^{-1}$, the values of p for (i) and (ii) differ by about one order of magnitude. I.e., effect (ii) has much more relevance than (i) and will be discussed here in detail.

4.3.2 The physiological submodel: constant temperature

As biochemical basis for the coupling problem we used a model of phytoplankton photosynthesis and photoadaptation derived earlier³:

$$\Pi(\gamma, I) = \frac{\mu_0}{\gamma} \cdot (1 - e^{-\alpha \gamma I / \mu_0}) \cdot e^{-\varepsilon \alpha \gamma I / \mu_0}, \quad (4.1)$$

where $\gamma = \gamma(t)$ follows from

$$\frac{d\gamma}{dt} = \gamma \cdot \mu_0 \cdot \left(e^{-\alpha \gamma I / \mu_0} - \frac{\gamma(t) - \gamma_-}{\gamma_+ - \gamma_-} \right) \cdot e^{-\varepsilon \alpha \gamma I / \mu_0}. \quad (4.2)$$

Here Π [$\text{gC} (\text{gChl})^{-1} \text{h}^{-1}$] is the instantaneous photosynthetic rate, I [W m^{-2}] the instantaneous light intensity (PAR) experienced by the cell, γ_- and γ_+ the minimum and maximum *Chlorophyll* equipments of a cell, respectively, ε the parameter of reversible photoinhibition, α the initial slope of the P - I curve and μ_0 [h^{-1}] a parameter closely related to the maximum physiologically admissible growth rate.

Whereas α , μ_0 , ε , γ_- and γ_+ are constant model parameters for constant temperature, $\Pi = \Pi(t)$ and $\gamma = \gamma(t)$ are variables which vary according to the above relations with $I = I(t)$ where t [h] is time.

While $\Pi = \Pi[\gamma(t), I(t)]$ reacts instantaneously on changes in I , γ follows the course of $I(t)$ with non-linear relaxation. Denoting steady-state variables by a starlet, for constant light the steady-state *Chlorophyll*-Carbon ratio, $\gamma^* = \gamma^*(I^*)$, is the solution of a transcendental equation and decreases monotonously with increasing I^* :

$$\gamma^* = \gamma_- + (\gamma_+ - \gamma_-) \cdot e^{-\alpha \gamma^* I^* / \mu_0}. \quad (4.3)$$

³ c.f. Baumert, H. - Int. Revue ges. Hydrobiol. **81** (1996) 1, 109-139

Figure 6 shows the solutions of (14) and (16) for a selected example species together with the laboratory observations under constant temperature.

4.3.3 The physiological submodel: variable temperature

The model presented above (see also *Baumert 1996*) contains the parameter μ_0 . This is a bulk quantity which consists of various elementary physiological parameters like, e.g., the molecular weight of *Chlorophyll-a*, efficiency measures of the primary photoreactions of photosynthesis, and (reciprocal value of) the reaction time constant of the two dark reactions of the Z-scheme of photosynthesis relevant for the present model. These dark reactions are enzymatical reactions and therefore strongly dependent on temperature. The temperature dependence is well known from enzyme kinetics and given by the mean kinetic energy of molecular motions as it follows from the Arrhenius law as follows (also known as Maxwell's law):

$$\tau^{-1} \propto \mu_0 \propto e^{-E/k \cdot T} \quad (4.4)$$

where here k is Boltzmann's constant, E the activation energy of the enzyme under consideration, and T the absolute temperature, i.e. $T = T_0 + T_C$, with the Celsius temperature T_C and $T_0 = 273^\circ$ Kelvin. Because of the property $T_C \ll T$, a Taylor expansion can be used to simplify (17):

$$\tau^{-1} \propto \mu_0 \propto e^{E \cdot T_C / k \cdot T_0^2} \quad (4.5)$$

where in practice one often finds $E/k T_0^2 \approx 0.062 \dots 0.068 (1^\circ\text{C})^{-1}$ (*Witt 1960, Aruga 1965, Eppley 1972, Crill 1977, Finenko 1978, Falkowski 1983*) corresponding to about half of an electron Volt (0.45 eV). Similar ideas as applied above to μ_0 have also been applied to the ε (A detailed inspection of the theory shows that this quantity is small and equal to the ratio of the time constants of the two dark reactions of the Z-scheme of photosynthesis; see *Baumert 1996*).

The basis for the calculation of the growth rate from the present model is the following energy balance equation,

$$\mu + r = \gamma \Pi \quad (4.6)$$

which equates the photosynthetically available energy, $\gamma \Pi$ (stored in various energy-containing compounds as result of the photosynthetic light and dark reactions) with the demand needed for cell (or population) growth, μ , and maintenance, r . We assume that there is a maintenance demand for the 'cell at rest' (i.e. without growth and cell division cycles), and another part describing the 'friction losses' during growth, i.e. energy which is not stored in new cells:

$$r = r_0 + \xi \cdot \mu. \quad (4.7)$$

This leads to the following expression for the growth rate in dependence on the parameter μ_0 which depends upon temperature as given by (18):

$$\mu(I, T_C) = \frac{1}{1 + \xi} \cdot \left[\mu_0 \cdot \left(1 - e^{-\alpha \cdot \gamma \cdot I / \mu_0} \right) e^{-\varepsilon \cdot \alpha \cdot \gamma \cdot I / \mu_0} - r_0 \right]. \quad (4.8)$$

Similar ideas as in (18) apply also to r_0 such that also this quantity is temperature dependent.

Figure 7 shows examples for the temperature dependence of the photosynthesis-light relation in the phytoplankton species *Oscillatoria redekei* in the temperature range 12° to 28° Celsius. The agreement between data and theory is surprisingly good.

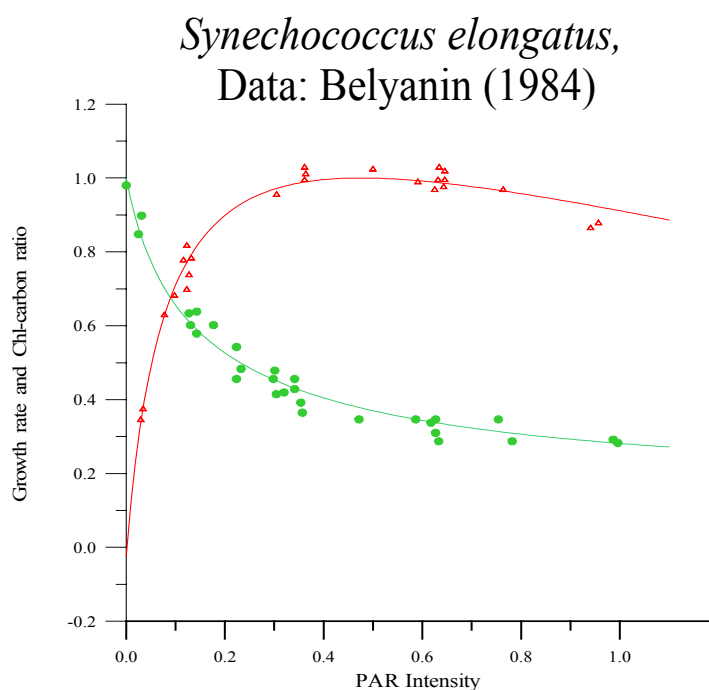


Figure 6:
Photosynthetic rate and Chlorophyll-Carbon ratio as functions of PAR intensity.

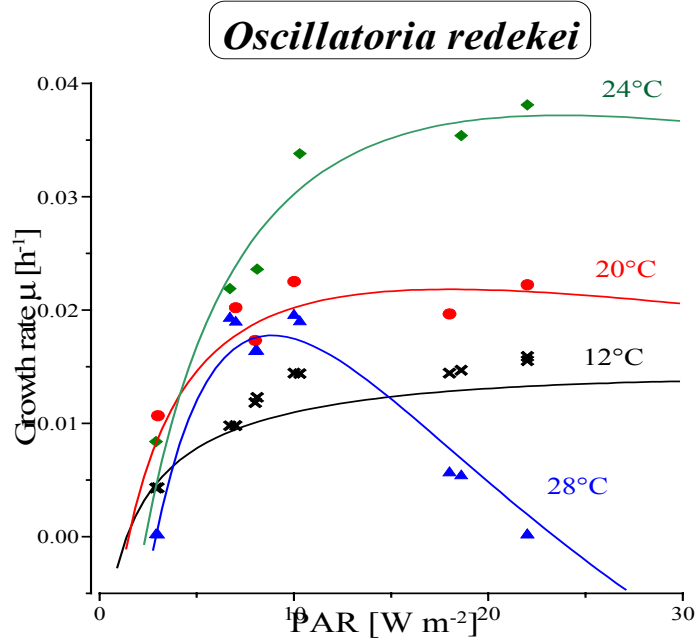


Figure 7:
Growth rates as functions of PAR intensity at various temperatures.
Symbols: laboratory observations from the literature; full lines: present model.

4.3.4 The hydrophysical submodel

For the physical model components we use existing knowledge and previous modelling results as follows. For simplicity of the presentation we assume constant turbidity or transparency of the water body along the vertical, without limiting the generality of our considerations. The light field $I = I(z, t)$ is then prescribed by the Lambert-Beer law with constant light attenuation coefficient k_z [m^{-1}]:

$$\frac{dI}{dz} = -k_z \cdot I, \quad I(0) = I_0, \quad I(z) = I_0 \cdot e^{-k_z \cdot z}. \quad (4.9)$$

I_0 is the light intensity just below the surface. The cell depth $z = z(t)$ [m] depends on time due to turbulence,

$$\frac{dz}{dt} = w'(t) \quad (4.10)$$

where w' [m s^{-1}] is the fluctuating vertical velocity component and equal to the cell's velocity. We approximated w' for simplicity by a zero-mean, white-noise stochastic process (in the Stratonovich sense):

$$\langle w'(t) \rangle = 0 \quad (4.11)$$

$$\langle w'(t') \cdot w'(t'+t) \rangle = D \cdot \lim_{\tau_v \rightarrow 0} \frac{e^{-|t|/\tau_v}}{\tau_v} = 2 \cdot D \cdot \delta(t) \quad (4.12)$$

$$D = \tau_v \cdot \sigma_v^2 = \text{constant} = \int_0^\infty \langle w'(t') \cdot w'(t'+t) \rangle dt \quad (4.13)$$

Here $\delta(t)$ is Dirac's delta function, τ_v [s] the autocorrelation time of the Lagrangian velocity fluctuations (vanishing in the white-noise limit), σ_v [m s^{-1}] the r.m.s intensity of those fluctuations (diverging in the

white-noise limit), ϕ [$\text{m}^2 \text{s}^{-2}$] their autocorrelation function (degenerating to a delta function in the white-noise limit) and D [$\text{m}^2 \text{s}^{-1}$] the turbulent diffusivity.

4.4 INTEGRATED BIOLOGICAL-PHYSICAL MODELLING

The interaction between the biological and the physical submodels is obvious: The light intensity I in (17) for a cell at position z is given by the Lambert-Beer law, and the position $z(t)$ itself is given as a function of time by (18). Therefore the dynamics of the *Chl*-carbon ratio $\gamma = \gamma(t)$ in a cell moving turbulently on the vertical axis in inhomogeneous light and temperature fields can be summarized as follows,

$$\begin{aligned}\frac{d\gamma}{dt} &= \Psi(\gamma, I(z, t), T_c(z, t)) \\ T_c &= T_c(z, t) \\ I(z, t) &= I_0 \int_0^z k_z(z, t) dz \\ \frac{dz}{dt} &= w'(t)\end{aligned}\tag{4.14}$$

where

$$\Psi(\gamma, I, T_c) = \gamma \cdot \mu_0(T_c) \cdot \left(e^{-\alpha \cdot \gamma \cdot I / \mu_0(T_c)} - \frac{\gamma(t) - \gamma_-}{\gamma_+ - \gamma_-} \right) \cdot e^{-\varepsilon(T_c) \cdot \alpha \cdot \gamma \cdot I / \mu_0(T_c)}\tag{4.15}$$

Here the temperature distribution $T_c = T_c(z, t)$ results from the mixed-layer model, k_z is the light attenuation coefficient [1/m], and I_0 the immediate sub-surface PAR intensity as function of the time of day and season.

Systems like (22, 23) with the statistics of the stochastic forcing function $w'(t)$ given by (19 - 21) are called Langevin equations. For those systems the corresponding joint probability density function $W = W(\gamma, z, t)$ [m^{-1}] is given by the solution of the corresponding Fokker-Planck equation (FPE). In the special case of constant temperature and constant light attenuation coefficient the FPE for (22, 23) reads

$$\frac{\partial W}{\partial t} + \frac{\partial}{\partial \gamma} (\Psi W) - \frac{\partial}{\partial z} \left(D \frac{\partial W}{\partial z} \right) = 0.\tag{4.16}$$

From the solution $W = W(\gamma, z, t)$ one obtains easily the mathematical expectation value of γ by calculating the first moment:

$$\bar{\gamma} = \bar{\gamma}(z, t) = \int \gamma \cdot W(\gamma, z, t) d\gamma\tag{4.17}$$

Application of this procedure to the full equation (24) gives in particular an evolution equation for the mathematical expectation value of γ :

$$\frac{\partial \bar{\gamma}}{\partial t} - \frac{\partial}{\partial z} \left(D \frac{\partial \bar{\gamma}}{\partial z} \right) = \int \Psi(\gamma, ..) d\gamma - [\gamma \cdot \Psi \cdot W]_0^{\infty}.\tag{4.18}$$

As the states $\gamma = 0$ and $\gamma = \infty$ cannot be occupied by the system, the last term (the boundary term) in the right-hand side of (26) vanishes. In analogy to (26) one may derive an equation for $\sigma_\gamma^2 = \overline{\gamma^2} - \bar{\gamma}^2$ (and also for higher moments) as function of z and t through multiplication of (24) by γ^2 and subsequent integration. The application of a Taylor series expansion around $\gamma = \bar{\gamma}$ with the abbreviations

$\Psi' = \partial\Psi / \partial\gamma$, $\Psi'' = \partial^2\Psi / \partial\gamma^2$ etc. gives

$$\begin{aligned} \frac{\partial\bar{\gamma}}{\partial t} - \frac{\partial}{\partial z} \left(D \frac{\partial\bar{\gamma}}{\partial z} \right) &= \Psi(\bar{\gamma}, z) + \frac{1}{2} \cdot \sigma_\gamma^2 \cdot \Psi''(\bar{\gamma}, z) + \dots \\ \frac{\partial\sigma_\gamma^2}{\partial t} - \frac{\partial}{\partial z} \left(D \frac{\partial\sigma_\gamma^2}{\partial z} \right) &= 2 \cdot D \cdot \left(\frac{\partial\bar{\gamma}}{\partial z} \right)^2 + [2 \cdot \Psi'(\bar{\gamma}, z) - \bar{\gamma} \cdot \Psi''(\bar{\gamma}, z)] \cdot \sigma_\gamma^2 + \dots \end{aligned} \quad (4.19)$$

If higher-order terms are neglected, this system can be integrated, either analytically (using an iterative approximation approach) or numerically. We have studied the properties of the solutions and found, that for practically important situations it is sufficient to consider the first equation in (27) and to neglect the contributions stemming from second and higher order.

For practical applications in computational biological oceanography we therefore recommend to compute the mathematical expectation value of the *Chlorophyll*-carbon ratio and the phytoplankton biomass (in carbon units) by the following system of partial differential equations:

$$\begin{aligned} \frac{\partial\bar{\gamma}}{\partial t} - \frac{\partial}{\partial z} \left(v_t \frac{\partial\bar{\gamma}}{\partial z} \right) &= \bar{\gamma} \cdot \mu_0(T_C) \cdot \left(e^{-\alpha \cdot \bar{\gamma} \cdot I / \mu_0(T_C)} - \frac{\bar{\gamma} - \gamma_-}{\gamma_+ - \gamma_-} \right) \cdot e^{-\varepsilon(T_C) \cdot \alpha \cdot \bar{\gamma} \cdot I / \mu_0(T_C)} \\ \frac{\partial C}{\partial t} - \frac{\partial}{\partial z} \left(v_t \frac{\partial C}{\partial z} \right) &= [\mu_0(T_C) \cdot (1 - e^{-\alpha \cdot \bar{\gamma} \cdot I / \mu_0(T_C)}) \cdot e^{-\varepsilon(T_C) \cdot \alpha \cdot \bar{\gamma} \cdot I / \mu_0(T_C)} - r_0(T_C)] \cdot \frac{C}{1 + \xi} \quad (4.20) \\ \text{Chl} = \text{Chl}(z, t) &= \bar{\gamma}(z, t) \cdot C(z, t) \end{aligned}$$

Here we now have used instead of D the eddy diffusivity v_t computed using a turbulence model.

Although the derivation of the upper equation in (28) is not trivial, in comparison to traditional marine-ecological models this new procedure adds only one single differential equation.

Further detail of our approach may be found in ANNEX A to this Deliverable 26. Applications to a whole-lake ecosystem of Loch Lomond may be found in the Final Report to EUROLAKES WorkPackage 22.

5 PART III: PIRKANMAA REGIONAL ENVIRONMENT CENTRE

Calculation of nutrients, phytoplankton biomass and chlorophyll-a⁴

5.1 INTRODUCTORY NOTE

In this contribution to EUROLAKES WP05, equations for calculating nutrients, chlorophyll *a* and phytoplankton are presented. The differential equations represent local rates of change of concentration, due to non-hydraulic physico-chemical and biological processes. Further detail may be found in the Final Report to EUROLAKES WorkPackage 22 where also applications of the equations below are given.

The basic assumption is that phytoplankton is affected by nutrients, light and temperature as well as grazing. For that reason, simulation of nutrients (phosphorus and nitrogen), light and temperature dependencies as well simulation of zooplankton are discussed.

5.2 PHOSPHORUS

Phosphorus can be simulated either as dissolved reactive phosphorus or as total phosphorus. The equation for dissolved reactive phosphorus is the following:

$$\frac{dDRP}{dt} = \mu\alpha_{BP}B - \rho\alpha_{BP}B + \frac{\lambda_{P1}}{h} + \frac{\lambda_{P2}}{h} \quad (5.1)$$

where

DRP	=	dissolved reactive phosphorus concentration
t	=	time
μ	=	growth rate coefficient of phytoplankton, $f(T)$
α_{BP}	=	ratio of phosphorus to phytoplankton biomass
B	=	phytoplankton biomass
ρ	=	respiration coefficient of algae, function of temperature, $f(T)$
λ_{P1}	=	rate of aerobic release of phosphorus from sediment, $f(T)$
λ_{P2}	=	rate of anaerobic release of phosphorus from sediment, $f(T)$
h	=	thickness of the hydraulic element

The corresponding equation for total phosphorus simulation is the following:

$$\frac{dTP}{dt} = -\frac{\sigma_P}{h}TP^2 + \frac{\lambda_{P1}}{h} + \frac{\lambda_{P2}}{h} \quad (5.2)$$

⁴Authors of PART III:

Dr. Tom Frisk and Dr. Victor Podsechine

Eurolakes Deliverable:	D26
From Workpackage:	WP 05
FP5_Contract No.:	EVK1-CT1999-00004
Version:	
Date:	20.10.03

where

- TP = total phosphorus concentration
 σ_P = sedimentation coefficient of total phosphorus, $f(T)$
 λ_{P1} = rate of aerobic release of phosphorus from sediment, $f(T)$, ($\mu\text{g m}^{-2} \text{d}^{-1}$)
 λ_{P2} = rate of anaerobic release of phosphorus from sediment ($\mu\text{g m}^{-2} \text{d}^{-1}$)

5.3 NITROGEN

In the simulation of nitrogen, there are several options. One of them is to simulate the fractions of dissolved nitrogen, i.e. ammonium, nitrite, and nitrate fractions. Total nitrogen or biologically active nitrogen can be simulated as well. If the fractions are simulated, the following equations are used:

$$\frac{dN_1}{dt} = -\beta_1 N_1 + \rho\alpha_{BN} B - \mu\alpha_{BN} Bq_1 + \frac{\lambda_N}{h} \quad (5.3)$$

where

- N_1 = concentration of ammonia nitrogen
 β_1 = nitrification coefficient, $f(T)$
 α_{BN} = ratio of nitrogen to phytoplankton biomass
 q_1 = the share of nitrogen that phytoplankton takes in ammonia form
 λ_N = rate of nitrogen release from the sediment, $f(T)$

$$\frac{dN_2}{dt} = \beta_1 N_1 - \beta_2 N_2 - \mu\alpha_{BN} Bq_2 \quad (5.4)$$

where

- N_2 = concentration of nitrite nitrogen
 β_2 = nitrification coefficient, $f(T)$
 q_2 = the share of nitrogen that phytoplankton takes in nitrite form

$$\frac{dN_3}{dt} = \beta_2 N_2 - k_d N_3 - \mu\alpha_{BN} Bq_3 \quad (5.5)$$

where

- N_3 = concentration of nitrate nitrogen
 k_d = denitrification coefficient, $f(T)$
 q_3 = the share of nitrogen that phytoplankton takes in nitrate form

If biologically active nitrogen is simulated, the equation is the following:

$$\frac{dN}{dt} = -\frac{\sigma_N}{h} N^2 + \frac{\lambda_N}{h} - k_d N + k_f \mu B_2 \quad (5.6)$$

where

N	=	concentration of biologically active nitrogen (sum of nitrate, ammonia and nitrogen in phytoplankton)
σ_N	=	sedimentation coefficient of biologically active nitrogen, $f(T)$
λ_N	=	rate of release of nitrogen from sediment, $f(T)$
k_d	=	denitrification rate coefficient, $f(T)$
k_f	=	nitrogen fixation rate coefficient, $f(T)$
μ	=	growth rate coefficient of cyanobacteria
B_2	=	biomass of cyanobacteria

In estimation of the denitrification rate coefficient it must be borne in mind that only part of biologically active nitrogen is as nitrate.

If total nitrogen is simulated, the equation is the following:

$$\frac{dT_N}{dt} = -\frac{\sigma_{TN}}{h} T_N^2 + \frac{\lambda_N}{h} - k_d N + k_f \mu B_2 \quad (5.7)$$

where

TN	=	total nitrogen concentration
σ_{TN}	=	sedimentation coefficient of total nitrogen, $f(T)$

5.4 CHLOROPHYLL

Chlorophyll *a* concentration or phytoplankton biomass can be simulated, or biomass can be calculated on the basis of chlorophyll *a* concentration or vice versa, taking advantage of statistical equations.

The change of chlorophyll *a* concentration can be described as follows:

$$\frac{dCH}{dt} = \mu CH - \rho CH - \frac{\sigma_{CH}}{h} CH \quad (5.8)$$

where

σ_{CH}	=	chlorophyll <i>a</i> settling rate coefficient, $f(T)$
---------------	---	--------------------------------------------------------

Growth rate was calculated using a Michaelis-Menten type function:

$$\mu = \mu_{\max} \frac{DRP}{K_{DRP} + DRP} \times f(I) \quad (5.9)$$

where

$$\begin{aligned}\mu_{\max} &= \text{maximum growth rate coefficient of algae, } f(T) \\ K_{DPR} &= \text{half saturation coefficient of algae, } f(T) \\ f(I) &= \text{light limitation function}\end{aligned}$$

5.5 CARBON-BASED BIOMASS

Biomasses of planktonic algae and cyanobacteria can be simulated as follows:

$$\frac{dB_i}{dt} = \mu_i B_i - \rho_i B_i - \frac{\sigma_{Bi}}{h} B_i - D_i \frac{B_i}{\sum B_i} Z \quad (5.10)$$

where

$$\begin{aligned}B_i &= \text{biomass of algae } (i=1) \text{ or cyanobacteria } (i=2) \\ \mu_i &= \text{growth rate coefficient of algae } (i=1) \text{ or cyanobacteria } (i=2) \\ \rho_i &= \text{respiration rate coefficient of algae } (i=1) \text{ or cyanobacteria } (i=2) \\ \sigma_{Bi} &= \text{settling rate coefficient of algae } (i=1) \text{ or cyanobacteria } (i=2), f(T) \\ D_i &= \text{efficiency coefficient of grazing of algae } (i=1) \text{ or cyanobacteria } (i=2) \\ Z &= \text{zooplankton biomass}\end{aligned}$$

The growth rate coefficient is calculated in the following way:

$$\mu_T = \mu_{\max i} f_i(I) f_i(T) \min[f_i(P), f_i(N)] \quad (5.11)$$

or

$$\mu_i = \mu_{\max i} f_i(I) f_i(T) f_i(P) f_i(N) \quad (5.12)$$

where

$$\begin{aligned}\mu_{\max i} &= \text{maximal growth rate coefficient of algae } (i=1) \text{ or cyanobacteria } (i=2), f(T) \\ f_i(I) &= \text{light-dependence function of algae } (i=1) \text{ or cyanobacteria } (i=2) \\ f_i(P) &= \text{limitation function of phosphorus for algae } (i=1) \text{ or cyanobacteria } (i=2) \\ f_i(N) &= \text{limitation function of nitrogen for algae } (i=1) \text{ or cyanobacteria } (i=2) \\ f_i(T) &= \text{temperature-dependence function of nitrogen for algae } (i=1) \\ &\text{or cyanobacteria } (i=2)\end{aligned}$$

Here also Michaelis-Menten type function can be used:

$$f_i(P) = \frac{P}{K_{Pi} + P} \quad (5.13)$$

where

P = concentration of biologically available phosphorus
 K_{Pi} = half saturation constant of P for algae ($i=1$) or cyanobacteria ($i=2$)

5.6 BIOLOGICAL AVAILABILITY OF NUTRIENTS

The concentration of biologically available phosphorus is calculated on the basis of total phosphorus:

$$P = \beta TP - \alpha_{BP} \sum B_i \quad (5.14)$$

where

β = ratio of biologically active phosphorus to total phosphorus
 α_{BP} = ratio of phosphorus and the summed biomass of phytoplankton and cyanobacteria

For nitrogen:

$$f_i(N) = \frac{N_a}{K_{Ni} + N_a} \quad (5.15)$$

where

K_{Ni} = half saturation constant of N for algae ($i=1$) or cyanobacteria ($i=2$)
 N_a = concentration of biologically active nitrogen

If biologically active nitrogen is simulate, the concentration of biologically available nitrogen is calculated as follows:

$$N_a = N - \alpha_{BN} \sum B_i \quad (5.16)$$

where

N = concentration of biologically active nitrogen (eg. 3)
 α_{BN} = ratio of nitrogen and the summed biomass of phytoplankton and cyanobacteria

If total nitrogen is simulated, the concentration of biologically available phosphorus is calculated as follows:

$$N_a = \gamma TN - \alpha_{BN} \sum B_i \quad (5.17)$$

where

γ = ratio of biologically active nitrogen to total nitrogen
 α_{BN} = ratio of nitrogen and summed biomass of phytoplankton and total nitrogen

5.7 LIGHT LIMITATION AND LAKE OPTICS

The basic idea of the light-dependence function $f(I)$ has the shape of the Michaelis-Menten form function:

$$f_i(I) = \frac{I}{K_{li} + I} \quad (5.18)$$

where

I = light intensity
 K_{li} = half saturation constant of light for algae ($i=1$) and cyanobacteria ($i=2$)

If it is integrated between the depths z_1 and z_2 and Lambert's extinction law is taken into account the following equation is obtained:

$$f_i(I) = \frac{1}{\epsilon (z_1 - z_2)} \ln \left(\frac{\frac{K_{li} + e^{-\epsilon z_1}}{I_0}}{\frac{K_{li} + e^{-\epsilon z_2}}{I_0}} \right) \quad (5.19)$$

where

ϵ = extinction coefficient
 I_0 = light intensity on the surface

Another light dependence function has been presented by *Steele* (1962):

$$f_i(I) = \frac{I}{I_{oi}} \cdot \exp \left[1 - \frac{I}{I_{oi}} \right] \quad (5.20)$$

I_{oi} = the optimal light intensity for the growth of algae ($i=1$) or cyanobacteria ($i=2$)

If the equation of Steele (1962) is integrated in the same way as the Michaelis-Menten equation, the following equation is obtained:

$$f_i(I) = \frac{1}{(z_2 - z_1)\epsilon} \left[e^{\left(1 - \frac{Ioi}{I} e^{-\epsilon z_2}\right)} - e^{\left(1 - \frac{Ioi}{I} e^{-\epsilon z_1}\right)} \right] \quad (5.21)$$

The extinction coefficient can be calculated using statistical equations, e.g. the one presented by Jones and Arvola (1984):

$$\epsilon = 0.011 COL + 0.60 \quad (5.22)$$

where

COL = colour of water (mg Pt l⁻¹)

5.8 TEMPERATURE AND MATTER CONVERSION RATES

The most widely used temperature correction function was presented by Streeter and Phelps (1925):

$$K(T) = K(T_s) \theta^{T-T_s} \quad (5.23)$$

where

$K(T)$ = reaction rate coefficient at temperature T

$K(T_s)$ = reaction rate coefficient at temperature T_s

The problem in the model is that it is monotonous so that reaction rates are supposed to grow along with increasing temperature. However, biological processes have an optimum temperature above which reaction rate decreases. *Lassiter and Kearns* (1973) have presented a temperature correction function that is suitable for describing the growth of phytoplankton:

$$\mu(T) = \mu(T_o) e^{a(T-T_o)} \left[\frac{T_m - T}{T_m - T_o} \right]^{a(T_m - T_o)} \quad (5.24)$$

where

T_o = optimum temperature of growth

T_m = maximum temperature of growth

a = parameter

The generic temperature dependence function, suitable for chemical and biological reactions, presented by *Frisk and Nyholm* (1980) is the following:

$$K(T) = K(T_s) e^{\int_{T_s}^T \ln \Theta dT} \quad (5.25)$$

where

$K(T)$ = reaction rate coefficient at temperature T
 $K(T_s)$ = reaction rate coefficient at standard temperature T_s

Θ is a linear function of temperature:

$$\Theta = a_T + b_T T \quad (5.26)$$

On the basis of Eqs (25) and (26) the following formula can be obtained:

$$f(T) = \frac{e^{\left(\frac{a}{b} + T\right) [\ln(a+bT) - 1]}}{e^{\left(\frac{a}{b} + T_s\right) [\ln(a+bT_s) - 1]}} \quad (5.27)$$

5.9 ZOOPLANKTON

Zooplankton biomass can be calculated as follows:

$$\frac{dZ}{dt} = \mu_z Z - \rho_z Z \quad (5.28)$$

where

Z = zooplankton biomass
 μ_z = growth rate coefficient of zooplankton
 ρ_z = respiration rate coefficient of zooplankton

The growth rate coefficient can be calculated using the following equation:

$$\mu_Z = \mu_{Z_{\max}} \frac{\sum B_i - B_L}{K_B + \sum B_i - B_L} \quad (5.29)$$

where

$\mu_{Z_{\max}}$ = maximal growth rate coefficient of zooplankton
 B_L = critical value for the summed biomass of algae and cyanobacteria

K_B = half saturation constant of algae and cyanobacteria

5.10 SUPPLEMENTING STATISTICAL MODELS

Statistical models describing connection between phosphorus and chlorophyll concentration. P = total phosphorus concentration ($\mu\text{g l}^{-1}$), chl = chlorophyll a concentration ($\mu\text{g l}^{-1}$)

$$OECD (1982): \quad chl = 0.28 P^{0.96} \quad (5.30)$$

$$Ahl \& Wiederholm (1977) \quad chl = 50 \left(1 - e^{-0.0026P - 0.000102P^2} \right) \quad (5.31)$$

$$Edmondson \& Lehman (1981) \quad chl = 0.55P - 4.8 \quad (5.32)$$

$$Megard (1978) \quad chl = 0.58P + 4.2 \quad (5.33)$$

$$Jones \& Bachmann (1976) \quad \ln chl = 1.46 \ln(1.11P) - 1.09 \quad (5.34)$$

$$Dillon \& Rigler (1974) \quad chl = 0.073 \left(\frac{P}{0.9} \right)^{1.449} \quad (5.35)$$

$$Ahl \& Wiederholm (1977) \quad chl = 150 \left(1 - e^{-0.000867P - 0.000111P^2} \right) \quad (5.36)$$

$$Schindler et al. (1978) \quad chl = 1.19P - 7.3 \quad (5.37)$$

$$Sakamoto (1966) \quad chl = 0.0735P^{1.583} \quad (5.38)$$

6 LIST OF REFERENCES

- Ahl, T. & Wiederholm, T. 1977: Svenska vattenkvalitetskriteriet. Eutrofierande ämnen. Statens Naturvårdsverk PM 918. 124 p.
- Baumert, H. - Systems analysis of silica-diatom interaction. *Internat. Revue ges. Hydrobiol.* **64**, 4, (1979) 457 - 473
- Baumert, H. - On the theory of P - I curves, growth and light-dark adaptation in phytoplankton. Part I: constant temperature. *Int. Revue ges. Hydrobiol.* **81** (1996) 1, 109-139
- Dillon, P. J. & Rigler, F. H. 1974: The phosphorus-chlorophyll relationship in lakes. *Limnol. Oceanogr.* 19(5): 767-773.
- Edmondson, W. T. & Lehman, J. T. 1981: The effect of changes in the nutrient income on the condition of Lake Washington. *Limnol. Oceanogr.* 26(1): 1-29.
- Frisk, T. & Nyholm, B. 1980: Lämpötilan vaikutuksesta reaktionopeuskertoimiin vedenlaatumalleissa. (The effect of temperature on reaction rate coefficients in water quality models). *Vesitalous* 5: 24-27 (In Finnish).
- Garçon, V.C., Baumert, H., Schrimpf, W. and J.D. Woods (1993) - Fluctuations: a task package for the physicists. In: *Towards a Model of Ocean Biogeochemical Processes* (ed.: G.T. Evans und M.J.R. Fasham), *NATO ASI Series* Vol. I 10, 47 - 70, Springer-Verlag
- Henderson-Sellers B. 1987. *Engineering Limnology*. Pitman (rush translation)
- Huisman J. and Weissing, F.J. 1994. Light-limited growth and competition for light in well-mixed aquatic environments: an elementary model. *Ecology* **75**(2): 507-520

- Jones, J. R. & Bachmann, R. W. 1976: Prediction of phosphorus and chlorophyll levels in lakes. *J. Water Poll. Control Fed.* 48(9): 2176-2182.
- Jones, R. & Arvola, L. 1984: Light penetration and some related characteristics in small forest lakes in Southern Finland. *Verh. Internat. Verein. Limnol.* 22(2): 811-816.
- Kirk J.T.O. 1983. Light and photosynthesis in aquatic ecosystems. Cambridge. 401 pp.
- Lafforgue M. 1990. Modelisation du fonctionnement d'un ecosysteme lacustre: le lac d'Aydat. These de Doctorat presente a l'Ecole Nationale Supérieure des Mines de Paris. 253 pp.
- Lassiter, R.R & Kearns, D.K. 1973. Phytoplankton population changes and nutrient fluctuations in a simple aquatic ecosystem mode. In Middlebrook, Falkenborg and Maloney (Eds.): *Modelling the eutrophication process*, pp. 131-138.
- Maitland, P.S., Smith, B. D. and G. M. Dennis, The crustacean zooplankton of Loch Lomond. In: *Monographiae Biologicae* 44, ed. by P. S. Maitland, W. W. Junk publ. 1981, The Hague, 135 – 154
- Megard, R. O. 1978: Phytoplankton, photosynthesis, and phosphorus in Lake Minnetonka, Minnesota. *Limnol. Oceanogr.* 17(1): 68-87.
- OECD 1982: Eutrophication of waters: monitoring, assessment and control. Paris. 154 p.
- Pacanowski, R. C., and S. G. H. Philander, Parameterization of vertical mixing in numerical models of the tropical oceans, *J. Phys. Oceanogr.*, 11, 1443 - 1451, 1981.
- Pomeroy, P. P., Zooplankton in Loch Lomond: perspectives, predation and power. In: *The Ecology of Loch Lomond* (eds.: K. J. Murphy, M.C.M Beveridge and R. Tippet), Kluwer Academic, 1994, pp. 75 – 90
- Sakamoto, M. 1966: Primary production by phytoplankton community in some Japanese lakes and its dependence on lake depth. *Arch. Hydrobiol.* 62(1): 128.
- Saura, M. 1990: Metsälannoitus vesistöjen rehevöittäjänä. Vesi- ja ympäristöhallituksen monistesarja 270. 71 s.
- Schindler, D.W., FEE, E. J. & RUSZCZYNSKI, R. 1978: Phosphorus inputs and its consequences for phytoplankton standing crop and production in the experimental lakes area and in similar lakes. *J. Fish. Res. Board Can.* 35(2): 190-196.
- Steele, J.H. 1962. Environmental control of photosynthesis in the sea. *Limnol. Oceanogr.*, 7: 137 - 150.
- Streeter, H.W. & Phelps, E.B. 1925. A study of the pollution and natural purification of the Ohio river. *Public Health Bull.* 141. U.S. Public Health Bull 141. U.S: Public Health Service. 75 p.
- Stefan H. and Ford D.E. 1975. Temperature dynamics in dimictic lakes. *J. Hydraulics Div. ASCE*, 101, HY 1: 97-114.
- Szeligiewicz W. 1998. Phytoplankton blooms predictions: a new turn for Sverdrup's critical depth concept. *Pol. Arch. Hydrobiol.* 45: 5010-511
- Tassin B. 1986. Contribution a la modelisation ecologique du lac Lemane: Modeles physique et biogeo-chemique du lac. *These de Doctorat*, Ecole National des Ponts et Chaussées, Paris, France, 312 pp.
- Weissing F.J. and Huisman J. 1994. Growth and competition in a light gradient. *Journal of Theoretical Biology* 168: 323-336